

Biodistribution and Radiation Dosimetry of ^{18}F -Fluoro-A-85380 in Healthy Volunteers

Michel Bottlaender, MD, PhD¹; Héric Valette, MD¹; Dimitri Roumenov, MD¹; Frédéric Dollé, PhD¹; Christine Coulon, BS¹; Michèle Ottaviani, BS¹; Françoise Hinnen, BS¹; and Marcel Ricard, PhD²

¹Service Hospitalier Frédéric Joliot, Department of Medical Research, Division of Life Sciences, French Atomic Agency, Orsay, France; and ²Service de Physique, Institut Gustave Roussy, Villejuif, France

This study reports on the biodistribution and radiation dosimetry of 2- ^{18}F -Fluoro-3-[2(S)-2-azetidylmethoxy]pyridine (^{18}F -fluoro-A-85380), a promising radioligand for the imaging of central nicotinic acetylcholine receptors (nAChRs). **Methods:** Whole-body scans were performed in 3 healthy male volunteers up to 2 h after intravenous injection of 137–238 MBq ^{18}F -fluoro-A-85380. Transmission scans (3 min per step, 8 or 9 steps according to the height of the subject) in 2-dimensional mode were used for subsequent correction of attenuation of emission scans. Emission scans (1 min per step) were acquired over 2 h. Venous blood samples were taken up to 2 h after injection of the radiotracer. Urine was freely collected up to 2 h after injection of the radiotracer. For each subject, the percentage of injected activity measured in regions of interest over brain, intestine, stomach, bladder, kidneys, and liver were fitted to a monoexponential model, as an uptake phase followed by a monoexponential washout, or to a biexponential model to generate time-activity curves. Using the MIRD method, ten source organs were considered in estimating radiation absorbed doses for organs of the body. **Results:** Injection of ^{18}F -fluoro-A-85380 was clinically well tolerated and blood and urine pharmacologic parameters did not change significantly. The primary routes of clearance were renal and intestinal. Ten minutes after injection, high activities were observed in the bladder, kidneys, and liver. Slow uptake was seen in the brain. The liver received the highest absorbed dose. The average effective dose of ^{18}F -fluoro-A-85380 was estimated to be 0.0194 mSv/MBq. **Conclusion:** The amount of ^{18}F -fluoro-A-85380 required for adequate nAChR imaging results in an acceptable effective dose equivalent to the patient.

Key Words: ^{18}F -fluoro-A-85380; PET; dosimetry; central nicotinic receptors

J Nucl Med 2003; 44:596–601

The nicotinic acetylcholine neurotransmitter system plays a crucial role in the mediation of memory-learning, neurologic-neuropsychiatric diseases, drug addiction, and

control of pain (1). Degeneration of cells containing nicotinic acetylcholine receptors (nAChRs) has been observed in several neurodegenerative diseases, including Parkinson's disease and Alzheimer's disease.

Imaging of nAChRs using PET could provide useful information on the integrity of the nAChR system in vivo. Therefore, it can be a potentially valuable technique for the diagnosis, follow-up, and study of the pathogenesis of several neurodegenerative diseases.

The development of radiolabeled tracers suitable as PET ligands for imaging nAChRs has been an important goal in the recent years. Among several developed compounds, the halogen derivatives of 3-[2(S)-2-azetidylmethoxy]pyridine (A-85380) are promising because of both their high affinity for the $\alpha_4\beta_2$ subtype and their low toxicity and lack of mutagenicity (2,3). 2- ^{18}F -Fluoro-3-[2(S)-2-azetidylmethoxy]pyridine (^{18}F -fluoro-A-85380) is being developed as a PET probe for the study of central nAChRs. This compound has been characterized in rodents and baboons (2,4). As part of phase I studies, this investigation was undertaken to assess the whole-body biodistribution of ^{18}F -fluoro-A-85380 and to calculate the associated radiation absorbed doses in healthy human volunteers.

MATERIALS AND METHODS

Radiosynthesis

Fluoro-A-85380 has been labeled with the positron emitter ^{18}F by no-carrier-added nucleophilic aromatic trimethylammonium-fluoro substitution by $\text{K-}^{18}\text{F-F-K}_{222}$ complex with (3-[2(S)-N-(tert-butoxycarbonyl)-2-azetidylmethoxy]pyridin-2-yl)trimethylammonium trifluoromethanesulfonate as a highly efficient labeling precursor, followed by trifluoroacetic acid removal of the Boc protective group (5). The total synthesis time was 50–53 min from the end of cyclotron ^{18}F production (end of bombardment [EOB]). Radiochemical yields, with respect to initial ^{18}F -fluoride ion radioactivity, were 68%–72% (decay corrected) and 49%–52% (non-decay corrected), and the specific radioactivities at EOB were 148–259 GBq/ μmol .

Subjects

The Medical Bioethics Committee of the Medical Center at the University of Paris XI approved this study. Three healthy male volunteers, with a mean age of 22 y (range, 21–23 y) and a mean weight of 74.2 kg (range, 69.3–79.8 kg) gave their written in-

Received Jul. 22, 2002; revision accepted Nov. 27, 2002.

For correspondence or reprints contact: Héric Valette, MD, Service Hospitalier Frédéric Joliot, Department of Medical Research, Division of Life Sciences, French Atomic Agency, 4 Place du Général Leclerc, F-91406 Orsay, France.

E-mail: valette@shfj.cea.fr

formed consent for participation in the study. The subjects were free of illness on the basis of screening by medical history, physical examination, serum chemical analysis, complete blood cell count, and urine analysis. They were nonsmokers as demonstrated by the negative plasma cotinine determination. A standard 12-lead electrocardiogram (ECG) was obtained for screening purposes. Before the start of the experiments, all volunteers were asked to urinate. During the PET experiment, ECG findings and blood pressure were continuously monitored from 10 min before to 10 min after the tracer injection. Serum chemical analysis, complete blood cell count and urine analysis were performed before and within 1 wk after completion of the PET study.

PET Imaging Procedure

During data acquisition, subjects were positioned supine with the arms alongside the body in the ECAT Exact HR+ PET scanner (CTI/Siemens, Knoxville, TN).

For each subject, a whole-body transmission scan was obtained before injection of the radioligand using 3 retractable ^{68}Ge rods (each with approximately 74 MBq). Transmission scans lasted 3 min per bed position (field of view, 15 cm), with 8 or 9 steps according to the height of the subject; they were used for subsequent correction of attenuation of emission scans.

Whole-body emission scans were performed (3-dimensional [3D] mode) after an intravenous bolus injection of 191 ± 50.9 MBq (range, 191–238 MBq)—that is, 1.73 ± 0.21 nmol of ^{18}F -fluoro-A-85380. One-minute step acquisitions, 8 or 9 steps for 1 scan (from the top of the head to the upper part of the thigh), were acquired over 2 h.

Urine Collection

All voided urine from the time of injection until 2 h after injection was collected. The urine was collected in a container, and the volume and time of micturition were recorded for all subjects. Three-milliliter urine aliquots were sampled and radioactivity was counted in an automatic γ -counter (model 5000; Packard Instrument Co., Downers Grove, IL). After the counting efficiency of the system had been determined, radioactivity measurements of the samples were corrected for physical decay and multiplied by the urine volume at the micturition time. The amount of radioactivity in the urine at the micturition time was expressed as percentage of the injected radioactivity (%ID). Because the vertebral bodies were clearly seen in all subjects and on all images, the presence of free ^{18}F -fluoride ion in the urine was checked. Five hundred microliters of urine were added to hydroxyapatite (10 mg) and incubated at 37°C for 30 min. The mixture was centrifuged at 3,000 rpm for 2 min. The supernatant was removed and counted. The pellet was washed with 500 μL distilled water and centrifuged again. The water layer and the pellet were counted.

Blood Collection

Twenty-four venous blood samples were taken at designated time points up to 120 min after injection. For each blood sample and each corresponding plasma sample obtained by centrifugation (5 min at 3,000 rpm), the amount of radioactivity in 100- μL aliquots was counted in an automatic γ -counter as above. The radioactivity measurements of the samples were corrected for physical decay.

^{68}Ge -Germanium Cylinder and Determination of Calibration Factor

To obtain an accurate factor for the conversion of ECAT counts to megabecquerels of radioactivity, a ^{68}Ge cylinder (radius, 10 cm;

length, 20 cm) was imaged with the PET scanner. A volume of 6,283 mL water was mixed with 27.75 MBq ^{68}Ge . An emission scan was acquired for 1 h in 3D mode. Cylinder emission data were reconstructed into a coronal image of the cylinder using the same method as for patient data reconstruction. A region of interest (ROI) was drawn over the entire PET image of the cylinder, and the total counts per second in the cylinder were determined. One count per second was found to be equivalent to 11.5 MBq/mL in 3D mode.

PET Data Analysis

The datasets acquired in 3D mode were corrected for scatter using a model-based correction allowing the simulation of the map of single scatter events. This method uses the map of attenuation coefficients and the image of activity concentration to compute the sinogram of single scatter events using the Klein–Nishima formula (6). Raw positron emission data were reconstructed using the ordered-subsets expectation maximization (OSEM) algorithm in the transaxial format with segmented attenuation correction (7). All reconstructions and image analyses used CAPP software, version 7/1 (CTI/Siemens). Two-dimensional or 3D views were assembled with bed position overlap (12 tomographic slices) and smoothed with a gaussian kernel of 5-mm full width at half maximum. All OSEM reconstructions were performed with 4 iterations and 8 subsets. The images were attenuation corrected using the transmission data collected over the same region of emission imaging.

Because the formalism used to perform absorbed dose calculation is based on the MIRD model (8), all source organs must be first identified from the reconstructed images. ROIs were then drawn over all organs presenting a significant uptake to construct time–activity curves. ROIs were drawn by an experienced investigator on the earliest emission image for liver, abdominal area (including upper and lower large intestine wall as well as small intestine), spleen, kidneys, vertebral bodies, and bone marrow (red); for brain and urinary bladder they were drawn on the emission image obtained 2 h after injection of ^{18}F -fluoro-A-85380. The shapes and sizes—that is, number of pixels—were kept constant for all individual patients. To determine the biologic clearance of ^{18}F -fluoro-A-85380, the activity was decay corrected back to the time of injection and time–activity curves were obtained.

Dosimetry

For dosimetry analysis, using the radioactive concentration (in MBq/mL) extracted from the quantitative images, the total activity contained in each source organ was assessed according to the standard-man model defined by Cristy and Eckerman (9). A new set of data, which depicts the behavior of source organ activity according time, was then generated. Data were fitted (least-square method) as follows: a monoexponential decline of radioactivity for upper large intestine and lower large intestine; a biexponential decline for liver, spleen, and kidneys; an uptake phase followed by a monoexponential decline for the brain and the red bone marrow; a monotonic increase for the bladder followed by a complete micturition at 120 min after injection. For all of these organs, the residence times (in h) were calculated by dividing the area under the time–activity curves by the injected dose. MIRDOSE3 software (10) was then used to estimate the mean absorbed dose by all organs included in the phantom due to the activity contained in the source.

Because healthy volunteers have been used in this study, the concept of effective dose must be used to express the risk encoun-



FIGURE 1. Whole-body coronal image of ^{18}F -fluoro-A-85380 distribution in healthy volunteer (subject 1, 1-min acquisition per step) obtained 92–104 min after intravenous injection of 200 MBq ^{18}F -fluoro-A-85380. Activity clears from other organs to kidneys and bladder over time.

tered. Preliminary calculations demonstrated that kidneys were receiving an absorbed dose as high as the most exposed organ (the liver). Therefore, according the recommendations of International Commission on Radiological Protection (ICRP) Publication 60 (11), a weighting factor, W_T , equal to 0.025 was applied to the kidneys (equal to that of the remainder of the body).

RESULTS

Biosafety

After injection of an average of 191 MBq ^{18}F -fluoro-A-85380 (range, 137–238 MBq; 1.7 nmol; range, 1.5–1.9

nmol), no adverse or subjective effects were noticed in any of the subjects. Their vital signs remained stable throughout the experiment. No significant changes in heart rate, blood pressure, or ECG findings were observed during the 10 min after injection of ^{18}F -fluoro-A-85380. Moreover, no meaningful changes were observed in any of the clinical laboratory assays performed on the blood and urine specimens obtained before and after administration of the radioligand (data not shown).

Biodistribution and Dosimetry

A whole-body image of 1 subject showing the biodistribution of radioactivity on injection of ^{18}F -fluoro-A-85380 at 92–104 min after injection is presented in Figure 1. Ten minutes after injection, high activity was clearly seen in the kidneys, intestines, and liver, and low activity was observed in the brain as well as in the lungs and the heart (Table 1). The images obtained between 1 and 2 h after injection showed that most of the radioactivity was distributed over the kidneys, bladder, liver, and intestines, whereas the uptake in the thalamus (a nAChR-rich region) became more visible at later times. A substantial and rather constant amount (0.4 %ID/100 g tissue from the beginning to the end of the PET acquisition) of radioactivity was seen on the vertebral bodies in all subjects. The radioactivity was rapidly increasing in the urinary bladder, indicating prompt excretion through the renal system. The mean measured urinary excretion at 2 h after injection was $22\% \pm 8\%$ of the administered activity. No free ^{18}F -fluoride ion was detected in the urine. No clear evidence of biliary excretion of ^{18}F -fluoro-A-85380 was seen on the images.

^{18}F -Fluoro-A-85380 was rapidly cleared from blood, and most of the activity is in the plasma portion. The average %ID remaining in the blood at 60 min after injection was 0.055 %ID/100 g tissue (range, 0.05–0.06 %ID/100 g tissue).

Penetration of ^{18}F -fluoro-A-85380 across the blood–brain barrier peaked at 25 min after injection and was followed by a slow clearance (Fig. 2). The average %ID was 0.182 %ID/100 g tissue (range, 0.16–0.196 %ID/100 g tissue). The thalamus showed the highest radioactivity (Fig. 3).

TABLE 1
Percentage Injected Dose of ^{18}F -Fluoro-A-85380 per 100 g Tissue for Subject 1

Time (min)	Lung	Heart	Spleen	Liver	Kidneys	Intestine	Brain	Urinary bladder	Bone marrow
2	0.313	0.519	1.072	1.072	1.074	0.668	0.138	0.874	0.112
13	0.174	0.274	0.583	0.583	0.870	0.525	0.182	1.099	0.176
25	0.138	0.211	0.424	0.424	0.658	0.510	0.197	1.795	0.189
36	0.113	0.155	0.316	0.316	0.535	0.460	0.195	2.327	0.148
47	0.098	0.140	0.299	0.299	0.446	0.461	0.188	2.560	0.215
59	0.086	0.113	0.238	0.238	0.392	0.471	0.177	2.766	0.128
70	0.075	0.103	0.198	0.198	0.341	0.334	0.165	2.813	0.135
81	0.068	0.082	0.182	0.182	0.298	0.391	0.152	2.809	0.095
92	0.060	0.082	0.158	0.158	0.272	0.427	0.140	2.698	0.112
104	0.054	0.072	0.155	0.155	0.248	0.411	0.127	2.618	0.097
115	0.048	0.062	0.140	0.140	0.226	0.409	0.116	2.515	0.077

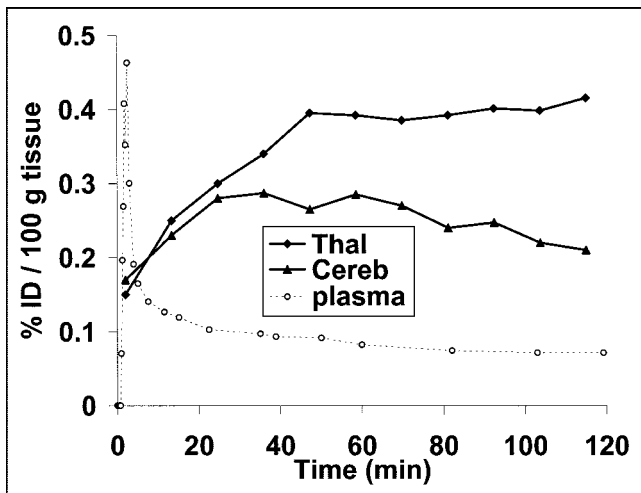


FIGURE 2. Thalamic (Thal), cerebellar (Cereb), and venous plasma (plasma) time-activity curves (decay corrected) after injection of ^{18}F -fluoro-A-85380 (200 MBq; subject 1). At 120 min after injection, thalamus-to-cerebellum ratio of radioactivity is 1.8.

The residence times were derived from the experimental organ distribution data and urine measurements of the 3 subjects (Table 2). The dataset of each subject was fitted independently. The residence time was highest for the remainder of the body, followed by the liver and the urinary bladder. The mean absorbed dose was then estimated using the MIRDOSE3 software (Table 3). Taking into account the weighting factor from ICRP Publication 60 (11), including the kidneys as previously described, the mean effective dose for the healthy adults was estimated to be 0.0194 mSv/MBq (range, 0.0178–0.0218 mSv/MBq).

DISCUSSION

The results of this study demonstrate the favorable biodistribution of ^{18}F -fluoro-A-85380 in human volunteers, with approximately 0.2 %ID/100 g tissue going to the brain. Moreover, our study demonstrates that ^{18}F -fluoro-A-85380 is a pharmacologically safe radioligand because it did not

TABLE 2
Residence Times (Hours) of ^{18}F -Fluoro-A-85380 for Each Source Organ

Source organ	Subject 1	Subject 2	Subject 3	Mean \pm SD
Liver	0.268	0.205	0.28	0.251 \pm 0.04
Spleen	0.014	0.011	0.013	0.013 \pm 0.002
Brain	0.062	0.053	0.069	0.061 \pm 0.008
Red bone marrow	0.25	0.15	0.146	0.182 \pm 0.059
Kidneys	0.07	0.05	0.062	0.061 \pm 0.01
Urinary bladder	0.108	0.267	0.072	0.149 \pm 0.1
Small intestine	0.118	0.06	0.053	0.077 \pm 0.036
ULI	0.065	0.04	0.037	0.047 \pm 0.015
LLI	0.04	0.031	0.029	0.033 \pm 0.006
Remainder	1.49	1.635	1.87	1.665 \pm 0.194

ULI = upper large intestine; LLI = lower large intestine.

produce any subjective or objective pharmacologic effects. In particular, ^{18}F -fluoro-A-85380 tracer did not have a significant effect on the volunteer's blood pressure, and ECG findings remained normal after tracer injection. Furthermore, ^{18}F -fluoro-A-85380 did not cause any significant changes in blood and urine parameters, supporting its lack of toxicity or pharmacologic effects.

The biodistribution of intravenously injected ^{18}F -fluoro-A-85380 showed that its main route of elimination is the renal system. This was expected because the tracer is highly hydrophilic (octanol buffer partition coefficient $\log P = -1.05$; M. Bottlaender, unpublished data, 2001). No significant defluorination of the tracer could be detected with the hydroxyapatite method. The amount of ^{18}F -fluoro-A-85380 in the liver and kidneys was initially high (1 %ID/100 g tissue), but the clearance of ^{18}F -fluoro-A-85380 in these organs was also rapid. The amount of ^{18}F -fluoro-A-85380 in the intestine decreased slowly during the first 80 min after injection and then increased slowly, perhaps reflecting the transit into the intestine. The uptake of radioactivity in the vertebral bodies was rather different than that observed after injection of ^{18}F -fluoride ion (12). Therefore, it is possible that ^{18}F -fluoro-A-85380 binds to the α_4 nicotinic subunits that are present in the human osteoblasts (13).

Regarding the estimation of energy deposition, the value of the calculated effective dose is in good agreement with the value given in ICRP Publication 80 of the ICPR (14) (1.9×10^{-2} mSv/MBq for adult population), which relates to the use of ^{18}F -FDG. This result can be explained by the fact that ^{18}F has a major contribution in the determination of residence time because of its short physical half-life. So, even when the behavior of the active molecule is significantly different, the impact of its biologic half-life may be less contributive. From the radiation protection point of view, dosimetric estimation for ^{18}F -fluoro-A-85380 remained well within the range of doses acceptable in clinical nuclear medicine studies. On the basis of the average effec-

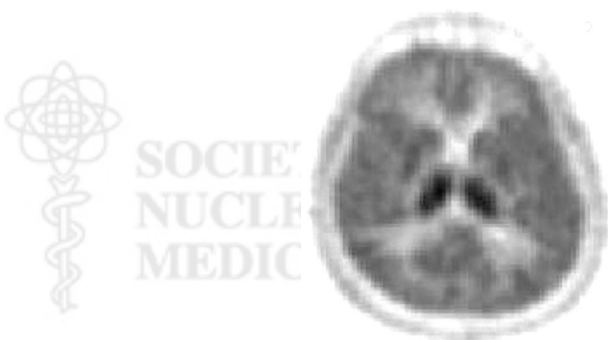


FIGURE 3. Late (one 5-min image, 120 min after injection) distribution of ^{18}F -fluoro-A-85380 in brain. Thalamus has highest uptake; in other structures, distribution is rather uniform.

TABLE 3
Mean Radiation Absorbed Dose Estimates (mGy/MBq) for ¹⁸F-Fluoro-A-85380

Target organ	Subject 1	Subject 2	Subject 3	Mean ± SD
Adrenals	1.49E-02	1.37E-02	1.60E-02	1.49E-02 ± 1.15E-03
Brain	1.29E-02	1.13E-02	1.43E-02	1.28E-02 ± 1.50E-03
Gallbladder wall	1.82E-02	1.62E-02	1.89E-02	1.78E-02 ± 1.40E-03
LLI wall	3.67E-02	3.24E-02	2.95E-02	3.29E-02 ± 3.62E-03
Small intestine	3.69E-02	2.49E-02	2.37E-02	2.85E-02 ± 7.30E-03
Stomach	1.22E-02	1.19E-02	1.35E-02	1.25E-02 ± 8.50E-04
ULI wall	4.01E-02	2.85E-02	2.77E-02	3.21E-02 ± 6.94E-03
Heart wall	1.11E-02	1.12E-02	1.30E-02	1.18E-02 ± 1.07E-03
Kidneys	5.25E-02	3.90E-02	4.75E-02	4.63E-02 ± 6.83E-03
Liver	3.90E-02	3.07E-02	4.06E-02	3.68E-02 ± 5.31E-03
Lungs	9.99E-03	9.99E-03	1.16E-02	1.05E-02 ± 9.30E-04
Muscle	1.00E-02	1.06E-02	1.12E-02	1.06E-02 ± 6.00E-04
Pancreas	1.45E-02	1.37E-02	1.58E-02	1.47E-02 ± 1.06E-03
Red marrow	2.74E-02	2.02E-02	2.06E-02	2.27E-02 ± 4.05E-03
Bone surfaces	1.95E-02	1.58E-02	1.68E-02	1.74E-02 ± 1.91E-03
Skin	7.28E-03	7.71E-03	8.55E-03	7.85E-03 ± 6.46E-04
Spleen	2.18E-02	1.82E-02	2.11E-02	2.04E-02 ± 1.91E-03
Testes	9.27E-03	1.13E-02	1.07E-02	1.04E-02 ± 1.04E-03
Thyroid	8.85E-03	9.34E-03	1.07E-02	9.63E-03 ± 9.58E-04
Urine bladder wall	6.16E-02	1.39E-01	4.49E-02	8.18E-02 ± 5.02E-02
Total body	1.19E-02	1.17E-02	1.26E-02	1.21E-02 ± 4.73E-04

LLI = lower large intestine; ULI = upper large intestine.

tive dose of 0.0194 mSv/MBq derived from the results of this study, both patients and human volunteers could be investigated with a multiinjection protocol for the quantification of central nAChRs.

Up to 185 MBq ¹⁸F-fluoro-A-85380 gives an average effective dose of approximately 4.3 mSv. This amount of radioactivity is adequate for PET imaging and gives an effective dose comparable to that delivered during a typical ¹⁸F-FDG examination. In addition, an effective dose equivalent of 5 mSv has been reported as the average effective dose equivalent per patient from nuclear medicine procedures in Europe (15). ICRP Publication 62 (16), which is dedicated to the radiologic protection in biomedical research, defines the level of risk corresponding to a given effective dose. Regarding the dose estimation performed in the framework of this study, the risk due to the administration of ¹⁸F-fluoro-A-85380 is then defined as minor to intermediate. For information, the level of natural irradiation in Europe typically ranges between 1 and 5 mSv/y.

CONCLUSION

Clinically and biologically, ¹⁸F-fluoro-A-85380 appeared to be a safe tracer. The biodistribution of ¹⁸F-fluoro-A-85380 in human volunteers demonstrated high and stable brain uptake. The dosimetry appeared favorable for clinical PET imaging. ¹⁸F-Fluoro-A-85380 has shown high affinity for nAChRs in animal studies and is now ready for testing on patients with neurodegenerative disease.

ACKNOWLEDGMENT

Part of this work was presented at the 49th Annual Meeting of the Society of Nuclear Medicine, Los Angeles, CA, June 15–19, 2002.

REFERENCES

- Gotti C, Fornasari D, Clementi F. Human neuronal nicotinic receptors. *Prog Neurobiol.* 1997;53:199–237.
- Valette H, Bottlaender M, Dolle F, et al. Imaging central nicotinic acetylcholine receptors in baboons with [¹⁸F]fluoro-A-85380. *J Nucl Med.* 1999;40:1374–1380.
- Valette H, Dollé F, Bottlaender M, Marzin D. Fluoro-A-85380 demonstrated no mutagenic properties in in vivo rat micronucleus and Ames tests. *Nucl Med Biol.* 2002;29:849–853.
- Valette H, Bottlaender M, Dollé F, et al. Characterization of the nicotinic ligand 2-[¹⁸F]fluoro-3-[2(S)-2-azetidylmethoxy]pyridine in vivo. *Life Sci.* 1999;64:PL93–PL97.
- Dolle F, Dolci L, Valette H, et al. Synthesis and nicotinic acetylcholine receptor in vivo binding properties of 2-fluoro-3-[2(S)-2-azetidylmethoxy]pyridine: a new positron emission tomography ligand for nicotinic receptors. *J Med Chem.* 1999;42:2251–2259.
- Watson CC, Newport D, Casey ME, et al. Evaluation of simulation-based scatter correction for 3D PET cardiac imaging. *IEEE Trans Nucl Sci.* 1997;44:90–97.
- Hudson HM, Larkin RS. Accelerated image reconstruction using ordered subsets of projection data. *IEEE Trans Med Imaging.* 1994;13:601–609.
- Loevinger R, Budinger TF, Watson EE. *MIRD Primer for Absorbed Dose Calculations.* New York, NY: The Society of Nuclear Medicine; 1991.
- Cristy M, Eckerman KF. *Specific Absorbed Fractions of Energy at Various Ages from Internal Photon Sources.* ORNL Report: ORNL/TM-8381 V1–V7. Oak Ridge, TN: Oak Ridge National Laboratory; 1987.
- Stabin MG. MIRDose: personal computer software for internal dose assessment in nuclear medicine. *J Nucl Med.* 1996;37:538–546.
- International Commission on Radiological Protection. ICRP Publication 60: Recommendations of the International Commission on Radiological Protection. *Ann ICRP.* 1991;21:493–502.

12. Hawkins RA, Choi Y, Huang SC, et al. Evaluation of the skeletal kinetics of fluorine-18-fluoride ion with PET. *J Nucl Med.* 1992;33:633–642.
13. Walker LM, Preston MR, Magnay JL, Thomas PB, El Haj AJ. Nicotinic regulation of c-fos and osteopontin expression in human-derived osteoblast like cells and human trabecular bone organ culture. *Bone.* 2001;28:603–608.
14. International Commission on Radiological Protection. ICRP Publication 80: Radiation dose to patients from radiopharmaceuticals—Addendum 2 to ICRP Publication 53. *Ann ICRP.* 1998;28:1–126.
15. Beekhuis H. Population radiation absorbed dose from nuclear medicine procedures in the Netherlands. *Health Phys.* 1988;54:287–291.
16. International Commission on Radiological Protection. ICRP Publication 62: Radiological protection in biomedical research. *Ann ICRP.* 1991;22:1–28.

